Biochimica et Biophysica Acta, 978 (1989) 223–230
Elsevier

BBA 74300

Wave-guide spectroscopy on planar lipid bilayers doped with hydrophobic ions

H.P. Braun and M. Vogel

Intitut für Physikalische und Theoretische Chemie der Technischen Universität München, Garching (F.R.G.)

(Received 21 July 1988)

Key words: Hydrophobic ion; Planar lipid bilayer; Wave guide spectroscopy

Wave-guide spectroscopy exploits the light pipe properties of planar lipid bilayers by propagating a light wave along the plane of the bilayer. Applying this technique to the optical absorption of chromophore in the membrane, results in an enhanced sensitivity when compared to normal incidence spectroscopy. This gain factor is of the order of 100 per mm optical path along the bilayer, thus transforming the weak absorbances in lipid membranes into easily measurable quantities. Wave-guide spectroscopy has been used to measure the adsorption isotherm of hydrophobic dipicrylamine ions in a phosphatidylcholine membrane. The adsorption isotherm is linear for low aqueous concentrations, in the micromolar range however, it changes into a sublinear dependence. The addition of an inert alkali salt to the electrolyte favours the adsorption of hydrophobic ions. Current saturation is observed with the transition to the sublinear isotherm. When using the time constant for current relaxation as an indicator of changes in the magnitude of the surface potential, it does not seem to vary with the additional dipicrylamine which adsorbs in the presence of high concentrations of alkali salt in the electrolyte. A compensation of hydrophobic charge by the alkali ions from the inert electrolyte is proposed.

Introduction

Since the detection of interfacially adsorbed hydrophobic ions in lipid membranes [1], the determination of their density has been of considerable interest. The ionic conductivity is closely related to the adsorbed interfacial charge density, because the ions being translocated across the membrane were either drawn from the interfacial layer of adsorbed charge or have to pass across it, thereby experiencing the local potential in the interfacial region. A phenomenon still under discussion is the presence of saturation effects observed with the transport of hydrophobic ions at high concentrations [1–3]. The low-voltage conductivity of hydrophobic ions reaches a maximum in the micromolar range. Simultaneously, the time constant for current relaxation increases, thereby significantly deviating from a purely exponential time course as observed for low ion concentrations. Several explanations are offered for this phenomenon suggesting the following.

(a) The translocation of an ion requires an empty binding site at the collecting interface. With increasing occupation of the binding sites, as envisaged for high ion concentrations, the probability for an ion translocation decreases [1].

(b) A structural change occurs with the ion adsorption, decreasing the membrane fluidity which in turn reduces the ionic mobility [3].

(c) A layer of immobile ions in front of the emitter screens a fraction of the external potential, thus lowering their transport velocity. This model proposes a space charge limited transport, thereby establishing a direct relationship between the surface potential and the time constant of current relaxation [4].

In order to find experimental evidence for one of the mechanisms we set out to determine the number of interfacially adsorbed ions under different electrostatic conditions, being controlled by the inert electrolyte.

Determination of the adsorbed hydrophobic charge

Electrical and optical methods were used to determine the adsorbed charge. The electrical methods [2,3] measure the charge being transferred upon the application of a high-voltage pulse. Since the potential applied forces the membrane out of equilibrium, we have to make several assumptions for the identity of the translocated charge with the interfacially adsorbed charge.

Correspondence: H.P. Braun, Institut für Physikalische und Theoretische Chemie der Technischen Universität Munchen, Lichtenbergstrasse 4, D-8046 Garching, F.R.G.

An outstanding advantage of the optical method is that it can be applied without disturbing the thermodynamical equilibrium of the membrane. However, optical methods are restricted to optically absorbing hydrophobic ions [5]. The major deficiency of absorption spectroscopy can be seen in the weak interaction of the the light with the minute amount of material contained in the bimolecular layer. Extremely small absorbances result from the interaction with the thin (5-nm) bilayer and ingenious optical spectrometers have been developed to resolve the absorbances in the 10^{-5} range [5,6]. Another difficulty of normal incidence spectroscopy in the present application arises from the fact that the probing light has to pass through several centimeters of the bulk electrolyte, which contains the absorbing ions [6].

The recently developed wave-guide spectroscopy [7] may help to overcome some of these drawbacks by considerably increasing the common path of interaction of light with the lipid film when propagating the light along the film for some millimeters. This gives rise to an enhanced optical absorption in the wave-guide mode by a factor of 100% per mm light path along the planar bilayer when compared to normal incidence spectroscopy. For details see Appendix B. Additionally, the optical path through the bulk electrolyte is shortened by the use of optical fibres bringing the probing light directly to the film.

Methods and Materials

As has been outlined in previous publications on wave-guide spectroscopy [7,8], the torus transition zone is used as an optical coupler between the fibres and the lipid film. This coupling element will contain more lipid material and probably more hydrophobic ions than the bimolecular lipid film itself. Since we do not know the exact shape of the torus transition zone and the distribution of hydrophobic ions therein we designed an experiment which eliminates the optical absorption in the bulk material. A wave-guide experiment has been developed where two light beams are guided in parallel across the lipid film differing only in their path length along the bimolecular area, as indicated in Fig. 1. The use of identical fibres results in identical optical coupling and absorption conditions in the torus transition region. Thus the ratio of the transmitted light intensities between the two optical branches reflects the optical absorption in the difference of the bimolecular light paths.

To ensure that only the light being transmitted along the lipid film in a wave-guide mode is measured, the optical fibres in the separator foil were arranged such that they form tangents to a spherically bulged lipid film [7]. Since only a guided wave can follow a curved ray path, unguided light is eliminated. The radiation

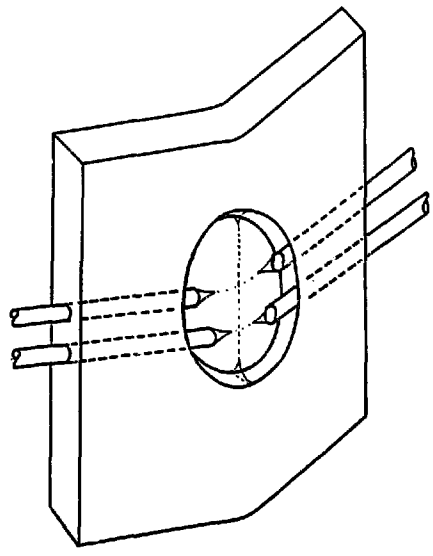

Fig. 1. Separator foil for double-beam wave-guide spectroscopy of planar lipid films. The foil contains mobile optical fibres in channels where the lipid material spontaneously forms horn-shaped optical coupling elements between the fibre ends and the bimolecular film.

loss which occurs with the bending of the membrane may not be attributed to the optical absorption of ions in the film. In order to evaluate the radiation loss, we measured the light transmission for a blank film in the inert electrolyte for later corrections [7].

For comparison of membrane absorptions in various electrolytes, we measured the transmission for each path with light which is not absorbed by the hydrophobic ions. Referring to this transmission, all changes in light intensity which do not originate from optical absorption of the hydrophobic ions will be eliminated. The path lengths along the bimolecular film were measured with a grid ocular, giving 1.80 mm for the long path, and 0,85 mm for the short one. The films were adjusted for maximum light transmission by exerting hydrostatic pressure from the electrolyte compartment facing the concave side. The bending radius of the separator foil was about 1.5 cm, causing an experimentally determined radiation loss, χ, of 3.8% mm^{-1} at a wavelength of 420 nm. Changes of the curvature during the experiment limited the resolution.

Experimental details. Fig. 2 shows a scheme of the optical device. Light from a 450 W dc xenon arc being filtered with a 420-nm interference filter of 25-nm transmission bandwidth (Schott) was simultaneously focused onto the flat surfaces of the entrance fibres of both branches (single-mode optical fibres, Siemens AG experimental type 1502-254, with 2-μm and 40-μm core- and cladding diameters, respectively). After passing the light along the lipid film, it was collected by similar fibres. Their endfaces were mounted in front of the blade of a vibrating reed chopper modulating the transmitted light of each branch by 100%, by switching one beam off and the other on. The chopped light intensity

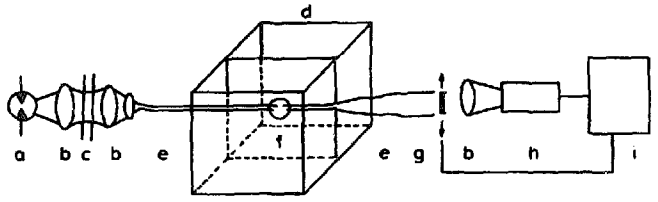

Fig. 2. Experimental set-up for double-beam wave-guide spectroscopy. (a) Xenon arc light source, (b) lenses, (c) heat protection and interference filters, (d) electrolyte cell, (e) optical fibres, (f) separator foil, (g) vibrating reed chopper, (h) photomultiplier and (i) lock-in amplifier.

was focused onto the photocathode of a XP1016 (Valvo) photomultiplier and the photo current was measured with a lock in amplifier (PAR HR8). When balancing the symmetry of the chopper for the two branches, this set-up allows for very accurate measurement of the difference in the transmitted light intensity. Blocking off one path measures the transmitted intensity of the other. For reference transmissions a 650-nm instead of the 420-nm filter was inserted. A molar absorption coefficient of $2.4 \cdot 10^4\ cm^{-1} \cdot M^{-1}$ according to Ref. 5 is used to convert absorbances into molar concentrations.

Optical alignment. The differential method will only work properly when both light paths have the same geometry. This requires that the four fibres must be adjusted to the same angle of incidence with respect to the membrane surface. A coarse alignment is obtained by varying the distance between the fibres until a maximum in the light transmission is observed. A very sensitive indicator for fine adjustment has been found in the electro-optic effect, which has been reported recently for wave-guide spectroscopy in undoped lipid films [7]. Upon application of a voltage pulse, one observes a modulation of the transmitted light intensity which reflects the polarity of the pulse. This signal changes phase when moving across the point of maximum light transmission and consequently is zero when the axes of both fibres point in the direction for peak transmission. For hydrophobic ions this signal is very strong, reflecting, optically, the equivalent of the electrically transferred ionic charge, as will be reported elsewhere. The relative amplitudes of the modulation signal in the two light paths are proportional to the optical path length, indicating that the set-up is aligned to wave-guide operation.

The lipid solution sponanteously forms a horn-shaped torus around the fibres. Its profile is determined by the contact angles of the solution between the bimolecular film and the flat fibre end. Identical fibres should, therefore, have identical torus' as coupling elements. Most of the light energy being coupled into the torus transition region is lost during the conversion of the incident light into the zero mode in which it can propagate along the bimolecular wave-guide. The efficiency of mode conversion is very sensitive to the shape of the coupling element. Accidental irregularities which may occur with the enclosure of lipid solution can be detected by a drastically changed coupling efficiency.

In order to judge the reliability of the data obtained by the differential method, we determined experimentally the extent to which the optical absorption from the bimolecular region is obscured by the torus. We measured the transmission spectrum for one light path with an optical multichannel analyzer (OMA II, Princeton Applied Research). The white light from the xenon arc was coupled into the input fibre and transmitted along the short light path. The endface of the collecting fibre was mounted in the focal plane of the polychromator (Jarrel Ash Mod. 1208) instead of the entrance slit. The spectral intensity was recorded with an ISIT 12051 (PAR) detector.

The magnitudes of the transient current and time constant of current relaxation upon the application of a voltage pulse were recorded with a current voltage converter and a Nicolet 4094/4562 digital oscilloscope. For details see Ref. 7. Data processing and the calibration of the wave-guide set-up is explained in Appendix C.

Membrane preparation. Black lipid films were prepared by applying the brush technique [9]. A solution of dioleoylphosphatidylcholine 18 : 1 in *n*-decane (Sigma) at a concentration of 2% w/v was used. Dipicrylamine (hexanitrodiphenylamine, Fluka Aurantia) was dissolved in the aqueous electrolyte with NaCl (Merck, p.a.) concentrations ranging from $10^{-}2$ M to 1 M.

Results

Fig. 3A shows the absorption spectra of dipicrylamine in the aqueous electrolyte and in asolectin-decane solutions. The absorption maximum shifts to the red with increasing concentration. Absorption experiments were performed in the broad absorption band at a wavelength of 420 nm, assuming a constant absorption coefficient for all dipicrylamine concentrations.

Fig. 3B represents the absorption spectrum of the lipid membrane including the two torus' and the bimolecular film which has been obtained with an optical multichannel analyzer. The 100% transmission curve for reference (a) was measured with an undoped dioleoylphosphatidylcholine (18 : 1) film in 0.1 M NaCl. The transmission curve for a similar film containing additionally $2 \cdot 10^{-6}$ M dipicrylamine is illustrated by curve b. The absorption spectrum (c) is calculated by matching curves (a) and (b) at 650 nm where dipicrylamine does not absorb. Since only 70% of the absorption is due to the torus region, the bilayer absorption can be recovered with high accuracy by the double-beam experiment. The high dark current of the vidicon detector did not allow the use of the polychromatic technique for low concentrations. We therefore

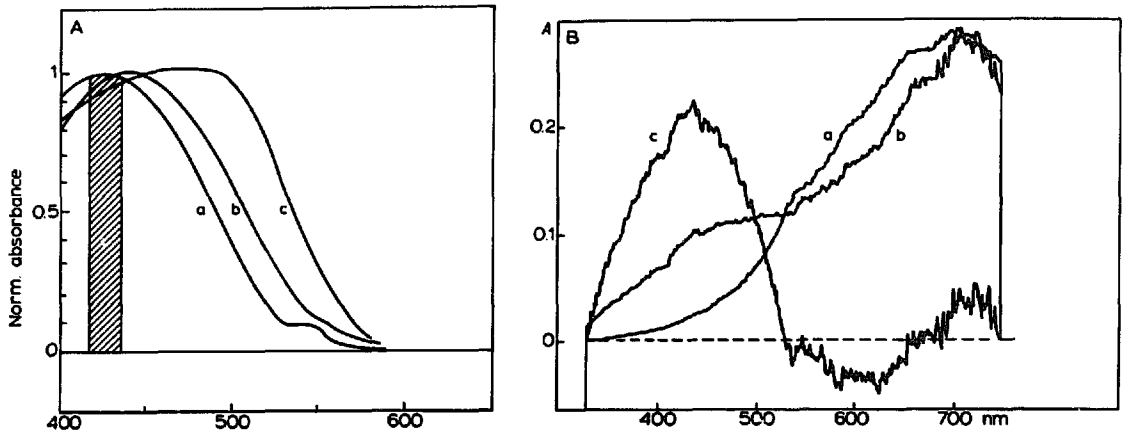

Fig. 3(A) Absorption spectra of dipicrylamine in aqueous and lipid-decane solutions. (a) Absorption spectrum of 10^{-6} M dipicrylamine in 0.1 M NaCl aqueous solution; (b and c) absorption spectra of 10^{-6} M dipicrylamine and 10^{-4} M dipicrylamine in 5% w/v asolectin-decane solution. (B) Absorption spectrum of a bimolecular film including the absorption from the bulky regions of the two torus segments (c). Trace a depicts the light transmission spectrum for an undoped membrane, trace b represents a membrane doped with $2 \cdot 10^{-6}$ M dipicrylamine in 0.1 M NaCl.

applied the more accurate method of comparing simultaneously the light transmissions in both light paths in a monochromatic experiment with a low-noise photomultiplier.

Fig. 4 shows the density of adsorbed hydrophobic ions per square centimeter of bimolecular area being determined at a wave length of 420 nm. The optical absorption was found to increase linearely with the ion concentration up to 10^{-7} M. Beyond this concentration, the slope of the adsorption curve is distinctly sublinear with a slope between 1/2 and 1/3, similar to the observations in Ref. 10. An outstanding observation is the marked increase of absorbed hydrophobic ions with increasing NaCl concentration, while the aqueous concentration of dipicrylamine ions is kept constant. The absolute number of adsorbed ions increases and the deviation from the linear adsorption isotherm shifts towards higher dipicrylamine concentrations. The total amount of adsorbed charge increases by 10 pmol $\cdot$ cm^{-2} for a change in the alkali concentration from 10^{-2} M to 1 M. Concentrations exceeding 10^{-5} M dipicrylamine could not be measured because the films did not become entirely thin; they always showed cluster like irregularities at the surface, especially in the presence of the dilute inert electrolyte.

Before interpreting the results, we have to ask whether the observation of enhanced ion adsorption with the inert electrolyte could be a peculiarity of wave-guide spectroscopy, influencing the guided mode via a change in the refractive index of the surrounding electrolyte. Examining Eqn. A-3 we see that an increase of the refractive index of the surrounding electrolyte increases the effective width of the guided mode and Eqn. B-3 then predicts a lower sensitivity. However, the reverse would be true when ions of the inert electrolyte adsorb into the membrane.

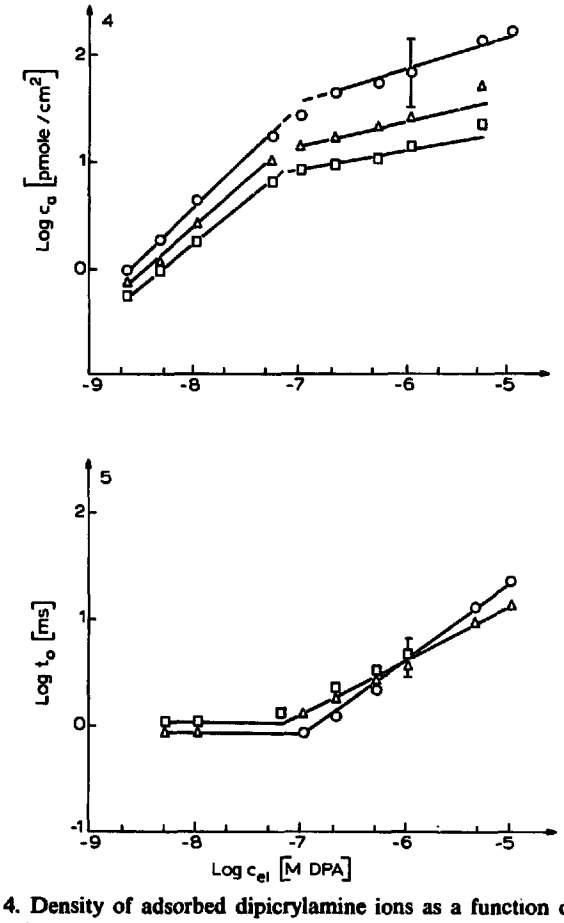

Fig. 4. Density of adsorbed dipicrylamine ions as a function of the dipicrylamine concentration in the inert electrolyte. The upper curve (○) is measured for a 1 M NaCl electrolyte, the middle (△) and lower curves (□) correspond to 0.1 and 0.01 M NaCl, respectively.

Fig. 5. Time constant t_0, of current relaxation, measured for the concentrations used in the experiments of Fig. 3. The upper curve (□) is for 0.01 and the lower curve is for 1 M NaCl. The time constants were derived on the basis of a hyperbolic time law.

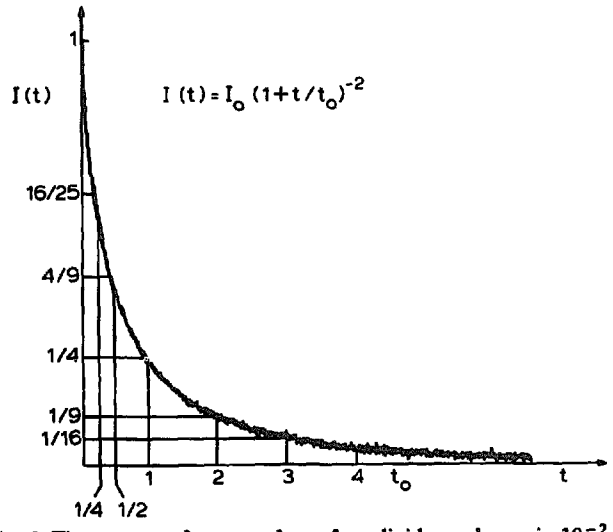

Fig. 6. Time course of current decay for a lipid membrane in 10^{-2} M NaCl electrolyte containing $5 \cdot 10^{-6}$ M dipicrylamine. The time course of the normalized current was fitted to a $(1 + t/t_0)^{-2}$ hyperbola with a time constant of 15 ms.

Current saturation, as indicated by an increased time constant of current relaxation, is observed when the adsorption isotherm becomes sublinear. Fig. 5 shows the time constants of current relaxation for a constant voltage of 50 mV and different dipicrylamine concentrations in the electrolyte. The time constants in the saturation regime were determined on the basis of a hyperbolic time law, which applies to the entire time range. The hyperbolic decay is a consequence of the quadratic current-voltage relationship as outlined in Ref. 4. Fig. 6 illustrates the agreement between the hyperbolic time law and experimental observation. Although the concentration of adsorbed ions varies with the concentration of the inert electrolyte, it does not significantly influence the time constants of current relaxation.

Discussion

The present results give valuable information about the mechanism of hydrophobic ion conduction in the current saturation regime. Comparing the three isotherms and their time constants of current relaxation, we find that the inert electrolyte facilitates hydrophobic ion adsorption with a negligible influence on the current saturation.

Thus, an occupation of more interfacial binding sites does not automatically lead to a decrease in conductivity. Therefore, the first proposition (a), explaining the saturating current by a limited number of binding sites [1], can be definitely excluded on the basis of the present results.

Considering the second explanation, a similar argument holds. The apparent membrane fluidity does not decrease, although more hydrophobic ions adsorb under the influence of the inert electrolyte. A determination of the ionic mobility on the basis of current relaxation experiments requires the knowledge of the driving electric field. Several transport models suggest that only a fraction of the external potential actuates the ion transport, yielding apparently lower ionic mobilities [12]. Thus, a reduction of the effective potential could simulate a lower ion mobility.

The third model [4] reveals a twofold action of the surface potential on the kinetics of ion transport. The surface potential controls the ratio of interfacially adsorbed (immobile) and desorbed (mobile) ions that carry the current. The immobile fraction of ions, in turn, will in part screen the external potential which drives the ions.

Ion adsorption and translocation is discussed on the basis of the three-capacitor model, where the adsorbed ions reside in minima of the potential curve being close to the electrolyte interfaces of the membrane. Ion adsorption within the minimum of the potential energy is interpreted in the sense of a reversible binding of the ions to the polar head group of lipid molecule. Only an ion that can afford the binding energy, $\psi - W$, will desorb from the interface and attain the energy level, W, from where it can be translocated across the membrane under influence of an external electric field. Thus, the physical significance of adsorption is expressed in different qualities of the adsorbed and desorbed ions. Only a desorbed ion can contribute to the current, whilst an adsorbed one is immobile not contributing to the current, but adding to the electric field by virtue of its charge. In thermal equilibrium, the ratio of adsorbed charge, q°, and desorbed mobile charge, q_m, in the interface is determined by Eqn. 1.

$$q_m/q^\circ = \exp -(\psi - W)/kT = \theta \tag{1}$$

The ion translocation is treated on the basis of a constant ion mobility, with an ion velocity being proportional to the effective driving field. In the derivation of the current–voltage curve for the saturation regime, the electrostatic field of the immobile charge is considered. This results in a partial screening of the external field driving the ions across the membrane with the consequence of lower drift velocities, and slower time constants for current relaxation, t_0.

$$t_0(c_a, U) = d^2/(\mu U) \cdot S_e(q^0) \tag{2}$$

The first bracket decribes the transit time for ions with a mobility, μ, across the membrane of thickness, d, by an external potential, U. The influence of the surface potential on t_0 via S_e, the electrostatic screening factor due to the adsorbed charges, is given by

$$S_e = (4/9)\theta d/l_a \tag{3}$$

where l_a denotes the thickness of the layer of adsorbed charges [4]. Eqn. 3 directly relates a change of the time constant of current relaxation to the change in the surface potential ψ in Eqn. 1.

Though it is found that more hydrophobic ions adsorb with higher concentrations of the inert electrolyte, the surface potential, being probed by the time constant of current relaxation, does not exhibit an adequate change. The additional charge being adsorbed under the influence of the inert electrolyte increases by 1 $\mu C/cm^2$ generating its dipolar potential in the membrane portion of the interface and not in the electrolyte [12]. Therefore, we can not attribute the reduction of the surface potential entirely to the screening length of the inert electrolyte [13,14]. Looking for further explanations for the reduction of the surface potential in the presence of the inert electrolyte, we consider a partial charge compensation by the inert electrolyte. Indications for such a mechanism were found on the application of wave-guide spectroscopy to undoped membranes in pure alkali electrolytes (work in progress).

Conclusions

Wave-guide spectroscopy is well suited to determine the number of adsorbed hydrophobic ions with a high degree of accuracy. The inert electrolyte, consisting of a solution of alkali ions, favours the adsorption of negative hydrophobic ions. Despite the fact that more hydrophobic ions adsorb under this condition, the time constant of current relaxation does not increase. This finding excludes the application of a model, where the saturation effects are attributed to the occupation of vacant binding sites at the collecting interface which were supposed to allow for an ion translocation. It turns out that electrostatic effects play an important role in the interfacial adsorption of ions. Indications for a compensation of negative hydrophobic charge by alkali ions from the inert electrolyte were found which could explain the observation of an enhanced ion adsorption without generating adequate change of the surface potential. This finding will shed some light on the interaction of the so-called inert electrolyte with the lipid membrane, demanding closer examination of the conduction mechanism and the mobile ion species in undoped membranes.

Acknowledgements

The authors wish to thank Professor M.E. Michel-Beyerle for many helpful discussions and Pauline Volk for preparation of the manuscript. This work was supported by the Deutsche Forschungsgemeinschaft, Sonderforschungsbereich 143.

Appendix A

Approximate analytical solutions for two important wave-guide parameters, the refractive index, N, and the effective thickness, d_{eff} are derived, which can be used instead of the numerical solutions of the transcendental mode equation.

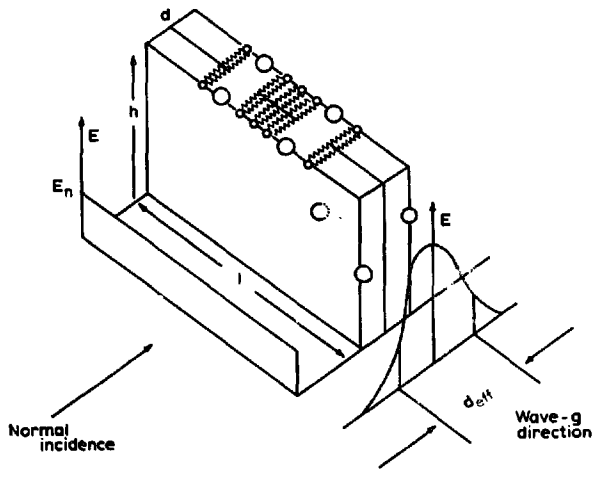

Fig. 7. Comparison of normal incidence and wave-guide spectroscopy on the basis of constant incident light power. The guided light wave is confined within d_{eff}, thus giving higher fields than in normal incidence, where the sample is probed with a plane wave extending across its whole surface and yielding lower fields.

As a consequence of the small d/λ ratio (1 : 100) the phases of the mode equation (Eqn. 4 in Ref. 7) are small, and the refractive index, N, is very close to the refractive index of the electrolyte n_e, thus we approximate N by

$$N = n_e + n \tag{A-1}$$

Using the small argument instead of the inverse-tangent function and neglecting terms of n^2 we obtain

$$n = [2\pi d(n_f^2 - n_e^2)/\lambda]^2/8n_e \tag{A-2}$$

where n_f and d denote the refractive index and the thickness of the lipid film. n shows a dispersion due to the wavelength dependence λ.

The second important parameter specifying a wave-guide is the effective width, d_{eff}. This denotes the lateral distance where the guided power density is decayed to $1/e$ of its maximum value; a rectangular field distribution of width d_{eff} carries the same power as the mode (see Fig. 7) [15].

$$d_{eff} = d + \lambda^2/[d(n_f^2 - N^2)\pi^2] = 0.1\lambda^2/d(n_f^2 - n_e^2) \tag{A-3}$$

Appendix B

The following describes an illustrative way of calculating the amplification factor of wave-guide spectroscopy [8]. The formulas were derived by assuming small optical absorption coefficients, that will negligibly modify the real part of the refractive index [16,17]. The

optical absorption of a constant number of absorbers measured by wave-guide spectroscopy is compared to the absorption obtained with normal incidence spectroscopy. Fig. 5 illustrates the geometry for both operations with a membrane of length l, thickness d and unit height with an refractive index n_f. This volume of the lipid film contains a concentration, c_a, of absorbers with a molar absorption coefficient ε.

For normal incidence spectroscopy, the optical density is proportional to the thickness d

$$OD_{ni} = n_f \varepsilon c_a d \tag{B-1}$$

We prefer to substitute n_f by n_e, because the phase velocity of the light is insignificantly influenced by the passage through the bimolecular film. In wave-guide operation the optical density for the same number of absorbers is proportional to the longer light path l, however, only light in the bimolecular volume d interacts with the absorbers, whereas the wave carries its light intensity with d_{eff}. Therefore, the optical density has to be corrected for the ratio d/d_{eff}

$$OD_{wg} = N\varepsilon c_a l d/d_{eff} = n_e \varepsilon c_a l d/d_{eff} \tag{B-2}$$

The ratio of optical densities for the different spectroscopic techniques yields the enhancement factor Q:

$$Q = OD_{wg}/OD_{ni} = n_f l/(Nd_{eff}) = l/d_{eff} \tag{B-3}$$

For actual application, operating at a wavelength of 420 nm in a 1 M NaCl electrolyte $n_e = 1.34$, with a lipid film of 5-nm thickness and $n_f = 1.45$, the effective width is 11 μm yielding a Q of 90 /mm and difference transmission ΔT of about 2% per mm bilayer for an interfacial density of 10 pmol/cm^2 dipicrylamine.

Eqn. B-3 was derived by assuming that the surrounding electrolyte is free of absorbing ions. In the present application, the wave propagates in a slightly absorbing electrolyte with a concentration c_e. The optical density being probed by the wave portion propagating in the electrolyte is

$$OD_{el} = n_e \varepsilon c_e l(d_{eff} - d)/d_{eff} = n_e \varepsilon c_a l \tag{B-4}$$

thus the ratio of wave-guide and bulk electrolyte absorption reads as

$$OD_{wg}/OD_{el} = c_a d/(c_e d_{eff}) \tag{B-5}$$

Using the data given in Refs. 4, 5 and 10 ($c_a/c_e = 10^5$), Eqn. B-5 predicts about 10-times more absorption in the bilayer than in the surrounding electrolyte. Considering a normal incidence experiment where the light has to pass through about 1 cm of the absorbing electrolyte, then the wave-guide technique reduces electrolyte absorption by a factor of 900.

Appendix C

Data processing and calibration of the wave-guide device

Eqn. C 1 gives the ratio, T, of transmitted light intensities, I, in the short and long light paths, respectively, for a doped membrane.

$$T(\lambda) = I_s/I_l = (I_{os}/I_{ol}) \cdot \exp - [\chi(l_l - l_s)] \cdot \exp - [c_a \varepsilon(\lambda) d/d_{eff}(l_l - l_s)] \tag{C-1}$$

We start with an undoped membrane in a pure electrolyte and measure the ratio of radiative losses, $R(\lambda)$, for 420 and 650 nm thereby eliminating the incident intensities I_0. Thus Eqn. C-1 reads as follows:

$$R(\lambda) = (I_{os}/I_{ol}) \cdot \exp - [\chi(l_l - l_s)] \tag{C-2}$$

After preparation of a new, doped membrane in an electrolyte containing dipicrylamine, we determine the ratio of transmitted light intensities in the branches for 650 and 420 nm wavelength. From the bulk absorption spectrum we know that the dye does not absorb at 650 nm, therefore this wavelength can be used as the 100% reference transmission.

$$T(420)/T(650) = [R(420)/R(650)] \cdot \exp - [c_a \varepsilon(420) \cdot (l_l - l_s)/d_{eff}] \tag{C-3}$$

Thus Eqn. C-3 contains only ratios of the transmitted light intensity which can be measured with high accuracy. These data need to be corrected for the absorption in the electrolyte according to Eqn. B-5.

Experimental determination of d_{eff} and calibration of the set-up

The electrically transferred charge at low concentrations of hydrophobic ions in the presence of a dilute inert electrolyte is used to calibrate the gain factor of the optical method. Which will be further used for the conversion into surface densities in the saturation regime, where the adsorption is governed by electrostatic effects. Fig. 4 shows that all isotherms coincide for low concentrations. Thus, the electrically translocated charge is assumed to be identical with the interfacially adsorbed charge at least in the low concentration regime.

For an aqueous concentration of $2 \cdot 10^{-8}$ M dipicrylamine, we determined electrically an adsorbed charge of 4 pmol/cm^2, which is monitored by wave-guide spectroscopy as a change in transparency of $1 \cdot 10^{-2}$. From these values the gain factor of wave-guide spectroscopy is calculated as 100/mm, which is used to convert the absorbance throughout the experiment.

Appendix D

Estimation of torus absorption

Wave-guides, being thicker than the wavelength, confine the light wave almost entirely inside their boundaries with the consequence that the effective thickness is very close to the physical thickness. Thus, for the torus we have $d/d_{eff} = 1$ along its length, l_{torus}. For the worst case estimation, we can approximate the torus by an equally sided triangle with the length of the fibre diameter (40 μm). (Calculations of the shape of the torus predict that the transition to the bimolecular film will occur along a much shorter distance [18]. The small magnitude of the coupling efficiency of 10^{-3} also indicates an abrupt transition between the bimolecular film and the fibre occurring within a distance of several tens of wavelengths, thus it is very likely that the torus occupies a small volume.) The ratio of optical densities between the bimolecular wave-guide and the torus may then be written as

$$OD_{wg}/OD_{torus} = c_a d(l_l - l_s)/(c_t d_{eff} l_{torus}) \qquad \text{(D-1)}$$

The concentration of hydrophobic ions in the bimolecular film, c_a, and in the membrane-forming solution in the torus, c_t, may be different. A 2% w/v solution has a density of $1.5 \cdot 10^{19}$ cm^{-3} lipid molecules, whereas for a bimolecular film we calculate a density of $6 \cdot 10^{20}$ cm^{-3} with 0.67 nm^2 specific area for a lipid molecule and a 5-nm thick double layer. Taking the same binding constant for hydrophobic ions for both states results in a 40-times lower ion concentration, c_t, for the torus. These data indicate that the optical absorption from the torus will exceed the absorption from 1 mm bilayer by less than a factor of 10.

References

1 Ketterer, B., Neumcke, B. and Läuger, P. (1971) J. Membr. Biol. 5, 225–245.
2 Andersen, O.S., Feldberg, S., Nakadomari, H., Levy, S. and McLaughlin, S. (1978) Biophys. J. 21, 35–70.
3 Bruner, L.J. (1975) J. Membr. Biol. 22, 125–141.
4 Braun, H.P. (1987) Biochim. Biophys. Acta 903, 292–302.
5 Wulf, J., Benz, R. and Pohl, W.G. (1977) Biochim. Biophys. Acta 465, 429–442.
6 Waggoner, A.S., Wang, C.H. and Tolles, R.L. (1977) J. Membr. Biol. 33, 109–140.
7 Braun, H.P., Winter, R., Karg, F.H. and Michel-Beyerle, M.E. (1984) Biochim. Biophys. Acta 773, 61–73.
8 Braun, H.P., Herrmann, R. and Michel-Beyerle, M.E. (1979) Z. Naturforsch. 34a, 1436–1455.
9 Müller, P., Rudin, D.O., Tien, H.T. and Wescott, W.C. (1962) Nature 194, 979–980.
10 Wang, C.C. and Bruner, L.J. (1978) J. Membr. Biol. 38, 1–21.
11 McLaughlin, S. and Harary, H. (1976) Biochemistry, 9, 1941–1948.
12 Wang, C.C. and Bruner, L.J. (1978) Biophys. J. 24, 749–764.
13 Benz, R. and Läuger, P. (1977) Biochim. Biophys. Acta, 468, 245–258.
14 Flewelling, R.F. and Hubbell, W.L. (1986) Biophys. J. 49, 531–540.
15 Tien, P.K. and Ulrich, R. (1970) J. Opt. Soc. Am. 60, 1325–1349.
16 Kane, J. and Osterberg, H. (1964) J. Opt. Soc. Am. 54, 347–352.
17 Ulrich, R. and Prettl, W. (1973) Appl. Phys. 1, 55–68.
18 White, S.H. (1972) Biophys. J. 12, 432–445.